Journal of Oceanography, Vol. 64, pp. 639 to 656, 2008

Surface Chlorophyll-a Dynamics in the Upper Gulf of Thailand Revealed by a Coupled Hydrodynamic-Ecosystem Model

ANUKUL BURANAPRATHEPRAT[1,2]*, TETSUO YANAGI[3], K. OLAF NIEMANN[2], SATSUKI MATSUMURA[4] and PRAMOT SOJISUPORN[4]

[1]*Department of Aquatic Science, Faculty of Science, Burapha University, T. Saensuk, A. Muang, Chonburi 20131, Thailand*
[2]*Department of Geography, University of Victoria, PO Box 3050, STN CSC, Victoria, British Columbia V8W 3P5, Canada*
[3]*Research Institute for Applied Mechanics, Kyushu University, Kasuga, Fukuoka 816-8580, Japan*
[4]*Department of Marine Science, Chulalongkorn University, 254 Phayathai Rd., Bangkok 10330, Thailand*

(Received 12 October 2007; in revised form 26 February 2008; accepted 12 March 2008)

Although plankton bloom incidents in the upper Gulf of Thailand (UGoT) have been reported, no dynamic investigation of the phenomenon has been conducted. To address this need, a simple pelagic ecosystem model coupled with the Princeton Ocean Model (POM) was employed to investigate seasonal variations in surface chlorophyll-a (chl-a) distributions to clarify phytoplankton dynamics in this area. The results revealed patterns of seasonal chl-a distribution that correspond to local wind, water movement and river discharge. High chl-a patchiness was found to be concentrated near the western coast following westward circulation near the northern coast developed during the northeast monsoon. During the southwest monsoon high concentrations were observed around the northeastern coast due to eastward flow. The simulated results could explain the seasonal shifting of phytoplankton blooms, which typically arise along the western and eastern coasts during the northeast and the southwest monsoons, respectively. Sensitivity analyses of simulated chl-a distributions demonstrate that water stability, including wind-induced vertical currents and mixing, plays significant roles in controlling phytoplankton growth. Nutrients in the water column will not stimulate strong plankton blooms unless upwelling develops or vertical diffusivity is low. This finding suggests an alternative aspect of the mechanism of phytoplankton bloom in this region.

Keywords:
· Ecosystem model,
· POM,
· chlorophyll-a distribution,
· Gulf of Thailand.

1. Introduction

The upper Gulf of Thailand (UGoT), a shallow coastal sea, is located south of central Thailand (Fig. 1). It is surrounded by land along the eastern, northern and western boundaries, and opens to the central GoT in the south. The area receives discharges from four main rivers including the Chaopraya River, the largest river in Thailand in terms of discharge volume. This river alone discharges approximately 13.22×10^3 km^3 of fresh water into the gulf annually (Wattayakorn, 2006). Seasonal variations in water density stratification exist resulting from variations in river discharge (Bunpapong and Piyakarnchana, 1987); the area can therefore be considered to be an estuary due to interaction of seawater and fresh water. Primary productivity of phytoplankton is high due to large nutrient loads introduced by the river drainage (Piyakarnchana *et al*., 1990). Consequently, this small area is highly productive and suitable for coastal aquaculture, especially shellfish farming (Chalermwat and Lutz, 1989). Green mussel, oyster and blood clam are intensely farmed throughout the area, with higher concentrations close to the river mouths. Fisheries and tourism are also important to both the local and national economies. Deterioration of the marine environment will unavoidably affect the standard and quality of life of local inhabitants.

* Corresponding author. E-mail: anukul@buu.ac.th

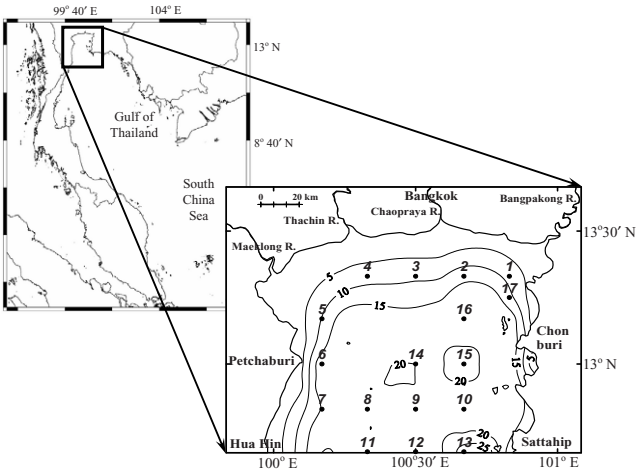

Fig. 1. Upper Gulf of Thailand. Contour lines represent water depth in meters and dots stand for observation points for optical and oceanographic data collections.

Eutrophication is one of several serious environmental problems in UGoT (Chongprasith and Srineth, 1998), owing to excessive nutrient loads from major rivers located along the northern coast. A survey (Rungsupa *et al*., 2003) reported over 90 red tide incidents, mostly concentrated in UGoT, from 1957 to 2001 with *Noctiluca scintillans* the most common species (50 times), following by *Trichodesmium erythraeum* (16 times) and *Ceratium furca* (9 times). Fortunately, the dominant blooming species do not produce toxin and are harmless to human health. Only one documented occurrence of Paralytic Shellfish Poisoning (PSP) in May 1983 has been reported. This event resulted in 63 people becoming ill and one death after consuming contaminated green mussels (*Perna veridis*) (Tamiyavanich, 1984). However, the heavy non-toxic blooms can, and do, result in dissolved oxygen depletion and high ammonia concentration in the water column, leading to potentially massive fish kills (Wattayakorn, 2006). The increasing trends of annual blooming incidents reported by the Pollution Control Department of Thailand (PCD) (http://www.marinepcd.org/coastalwater/wq10year.html) are an obvious indicator of a worsening problem. Escalation of the anthropogenic nutrient load has been blamed as the most important cause of the blooms, although there was no evidence of a systematic trend nutrient increase in the water column (Wiriwutikorn, 1996).

Blooming can be found all year round but in different locations—in the west and the east of UGoT during the northeast (November to January) and the southwest (May to August) monsoons, respectively (Lirdwitayaprasit *et al*., 1994). The most important factors, however, have not yet been clarified, although large nutrient loads have been linked to massive plankton blooms, especially during the wet season or the southwest monsoon season (Piemsomboon, 2003). Attempts have been made to investigate the relationship between water quality and plankton cell density. The results indicated that plankton abundance close to the river mouths is related to nutrient concentrations, while other factors such as temperature and salinity did not show any significant relationship (Lirdwitayaprasit *et al*., 2006). Blooming was not always found in high-nutrient, nearshore waters, but farther from the river mouths (Rungsupa *et al*., 2003) and offshore areas (Matsumura *et al*., 2006). This suggests that mechanisms related to plankton blooming are complex and that water quality alone cannot be used to describe the phenomenon.

Table 1. List of cruises to collect oceanographic data.

Cruise name	Date
CU-1	9–11 October 2003
CU-2	4–6 December 2003
CU-3	13–15 January 2004
CU-4	12–15 May 2004
CU-5	7–10 October 2004
CU-6	26–28 July 2005

This study focuses on an investigation of the relationship between surface chl-a distributions and environmental factors, using a numerical model for lower trophic levels of the marine ecosystem. Coupled with the Princeton Ocean Model (POM) (Blumberg and Mellor, 1987), the ecosystem model is used to simulate chl-a distributions in the study area. A diagnostic experiment was carried out using observed data conducted during the northeast and the southwest monsoons. This, therefore, is sufficient to represent the seasonal variations in chl-a distributions in the area. Calculated results were compared and verified against those of field observations. The distributions were carefully re-investigated using a sensitivity analysis, during which key influencing parameters including nutrient loads, discharges and wind magnitudes were modified. The main purpose of all experiments is to clarify the mechanism of surface chl-a dynamics and phytoplankton blooms in UGoT.

2. Field Observations

Sampling to assess the physical and biological properties was completed at 17 stations covering the entire area (Fig. 1). Due to the size of the area of interest, a sampling cruise took 3–4 days to complete. There were 6 cruises altogether, starting from October 2003 (CU-1) to July 2005 (CU-6) (Table 1). Salinity and temperature were probed in-situ employing a CTD, while water samples

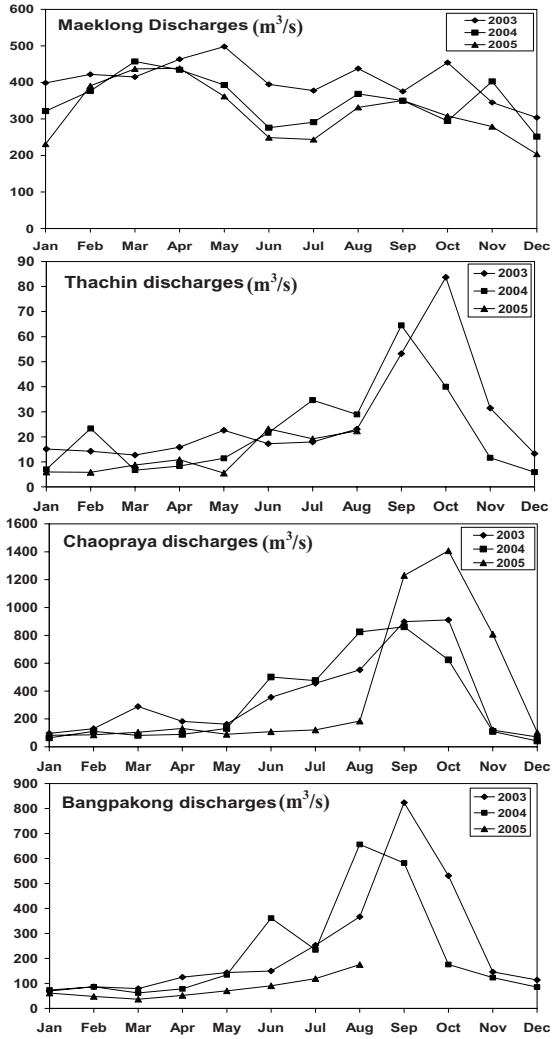

Fig. 2. Monthly mean discharges of four main rivers emptying into the head of the upper Gulf of Thailand.

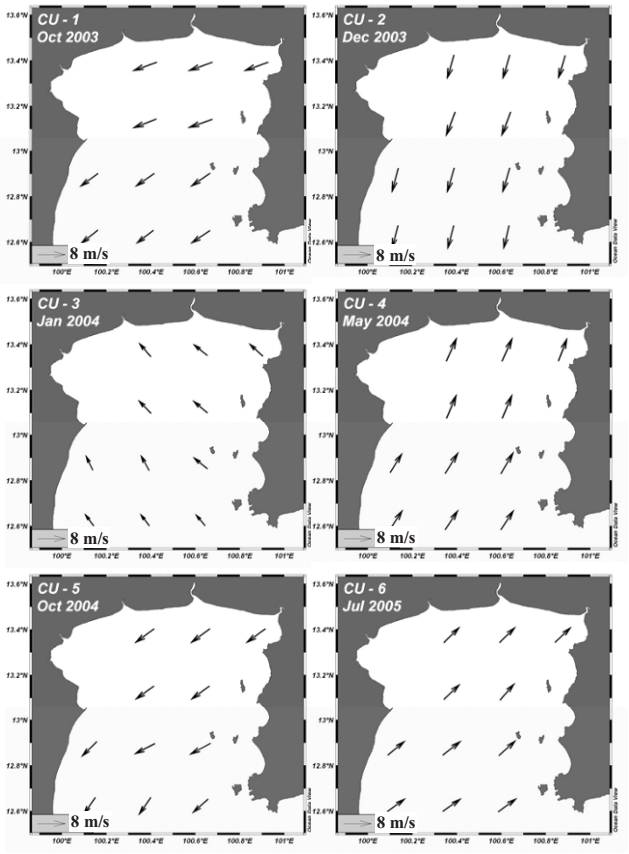

Fig. 3. Monthly mean winds of QuickScat data (http://www.ssmi.com) in the same months as observational cruises.

for chemical and biological analyses were collected using a Vandorn water sampler. Water samples were immediately filtered through a GF/F filter onboard, and then stored in a freezer for further analyses in the laboratory. Chlorophyll fluorescence was measured on the filtrate for chl-a (Strickland and Parsons, 1972), while the filtered water was analyzed for nutrients (ammonia, nitrate, nitrite, silicate and phosphate) with the use of a Skalar automated nutrient analyzer (Matsumura *et al*., 2006).

3. Circulation Model

Both circulation and ecosystem models were simultaneously operated, but only the circulation results are presented in this section. Details of the ecosystem model and biochemical results are included in Section 4 and Appendix. POM is used to simulate three-dimensional circulation. The governing equations of the model include conservation of mass and momentum, salinity, temperature and turbulence equations under the hydrostatic and Boussinesq approximations. The equations are written in a bottom-following, sigma coordinate system where vertical layers are scaled according to bottom topography. POM can take both barotropic and baroclinic forces into consideration by using the splitting technique. Time steps are separated into two different modes—a two-dimensional mode with a short time step of external wave speed (external mode) and a three-dimensional mode with a long time step of internal wave speed (internal mode). To maintain operational stability, both time steps are controlled under the Courant-Friedrichs-Levi (CFL) condition (Mellor, 1998). A vertical mixing coefficient is calculated in an imbedded second-moment turbulence closure submodel. The Smagorinski diffusivity is applied to estimate horizontal mixing coefficients. More details of the POM, including a mathematical description, are contained in Blumberg and Mellor (1987), and Mellor (1998).

To apply the circulation model to UGoT it was di-

Table 2. Tidal harmonic constituents used to calculate water elevation at the sea boundary.

Harmonic constituents	Huahin		Sattahip	
	Amplitude (cm)	Phase (deg)	Amplitude (cm)	Phase (deg)
K1	61.2	155.1	58.7	162.0
O1	39.0	119.2	29.3	112.0
M2	29.7	139.9	26.1	121.0
S2	15.3	212.8	12.3	192.0

vided horizontally into 124 × 102 grids in spherical coordinates with grid spacing 0.5 × 0.5 minutes in latitude and longitude, respectively. The vertical domain was set to 10σ-levels without logarithmic portions. The model uses bathymetry data from a 5-Minute Gridded Global Relief Data (ETOPO5) from the World Data Center for Marine Geology & Geophysics (http://www.ngdc.noaa.gov/mgg/global/relief/ETOPO5/). ETOPO5 is sufficient to represent the bathymetry of the area. This dataset has been used successfully in our previous studies (e.g., Buranapratheprat *et al*., 2002). Salinity and temperature profiled data, used as volume forcing, were obtained from field observations. Monthly means of daily discharges of four main rivers (Fig. 2), used to derive boundary conditions at the river mouths, were derived from data supplied by the Royal Irrigation Department (RID) of Thailand. Monthly averaged winds of QuickScat (http://www.ssmi.com) (Fig. 3) were used as an important surface driving force. QuickScat is one of the complete wind datasets available for the study area. Data points at every 0.25 degree are sufficient for model simulation because spatial variation of wind vectors is small. Tidal currents, as water elevations, were set to drive the water system through the sea boundary.

Discharge data of four main rivers, provided by RID, were derived from the conversion from water level into river flow, or stage-discharge relationships. This application is useable only where the disturbance due to tidal force is small, so the stations need to be located a distance upstream where the effects are lessened. Estimated data at stations closest to the river mouths, where the relationship between water level and river flow are still reliable, are used in the case of the Maeklong and the Chaopraya Rivers (Fig. 1). Due to strong tidal influence, especially during the dry season, an alternative method of estimation was necessary for the Bangpakong River discharges. Fortunately, this river has a very complete dataset of discharges in most sub-basins located upstream; therefore the summation of known and extrapolated values of unmeasured sub-basins are representative of the total discharge at the river mouth. Water flows through a water gate located downstream were used instead of real discharges due to strong tidal influences in the case of the Thachin River, the smallest river and a tributary of the Chaopraya. Although such data appear to be underestimated when compared to real discharges, they represent the most reliable data sources available. For the river boundary condition, discharge was transformed to a water level and added to the water elevation of computational grids at the river mouths, following the technique described in Kourafalou *et al*. (1996).

The ocean boundary in the south of the area is forced by tide via water elevations. Water levels in the east (Sattahip) and the west (Huahin) (Fig. 1) were first computed using a harmonic analysis technique. Four tidal constituents, namely K1, O1, M2 and S2, were considered in harmonic analysis where their amplitudes and phases at Sattahip and Huahin (Table 2) have been reported in Sojisuporn and Putikiatikajorn (1998). The intervening grid cells were populated using linear interpolation. During model operation, water elevations along the sea boundary were updated at every external time step under the radiation condition (Mellor, 1998). Components of velocities perpendicular to land boundaries were set to zero, while the radiation condition was also assigned at the sea boundary of the internal mode. The open boundaries for salinity, temperature, and turbulence parameters were set by a condition called "upstream advection" as defined in Eq. (1) (Mellor, 1998):

$$\frac{\partial T}{\partial t} + U\frac{\partial T}{\partial x} = 0, \tag{1}$$

where T is referred to those parameters; U and x are velocity and length perpendicular to the boundary, respectively; and t is time. Salinity and temperature are observed values which were fixed throughout model operation.

The model is operated using a technique called the robust diagnostic (Yanagi, 1999), where damping terms are introduced to the temperature and the salinity equations. These additional terms are $\gamma(T^* - T)$ and $\gamma(S^* - S)$, respectively. Here, γ is called the nudging constant ($=\Delta T_i/(86{,}400\text{ s} \times 5)$); ΔT_i is internal time step (300 s); and T^* and S^* are the observed water temperature and

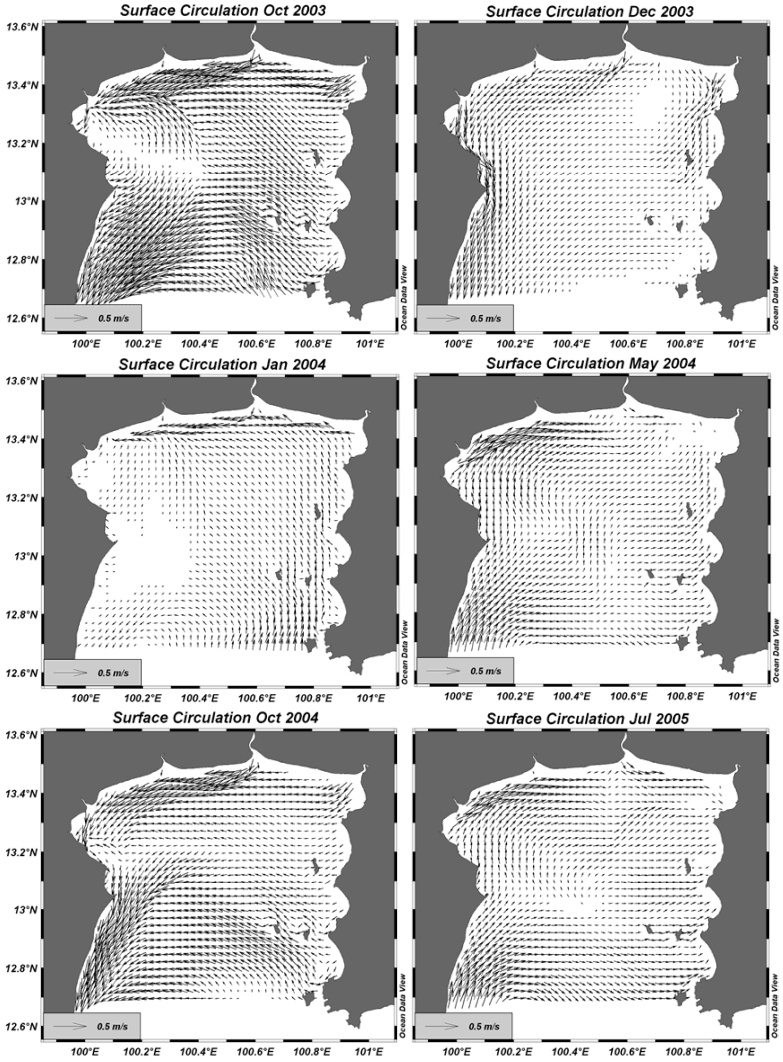

Fig. 4. Simulated surface velocity in the same months as all cruises.

salinity, respectively. In POM operation, the damping terms are added in the process of data updates before going to the next round of calculation.

General equations of complete three-dimensional Gauss function applied for the interpolation process are as follows:

$$\zeta = \frac{\sum_{i=1}^{n}(W \cdot \tau)}{\sum_{i=1}^{n} W}, \tag{2}$$

$$W = \exp\left\{-\frac{(r_i - x)^2}{I^2} - \frac{(r_j - y)^2}{J^2} - \frac{(r_k - z)^2}{K^2}\right\}, \tag{3}$$

where ζ is an interpolated parameter at any grid point; τ is observed data; n is the number of observed data points; x, y and z are interpolated grid positions (x and y are horizontal, and z is vertical); r_i, r_j and r_k are positions of observed data in x, y, and z directions, respectively. I and J are the horizontal decorrelation scales, set to 30 km, while K is that of vertical scale, set to 2 m. Temperature and salinity used as inputs for all computational grids are interpolated in three-dimensional space. On the other hand, wind and bathymetry are interpolated in two-dimensional space, so the vertical term on the right-hand side of Eq. (3) is excluded in this case.

The model was set to have no momentum fluxes generated by exchanges of heat and salt from the atmosphere or sea bottom because they are considered to be insignificant when compared to wind, discharges and tide. Seawater state was set at rest at the initial time of model

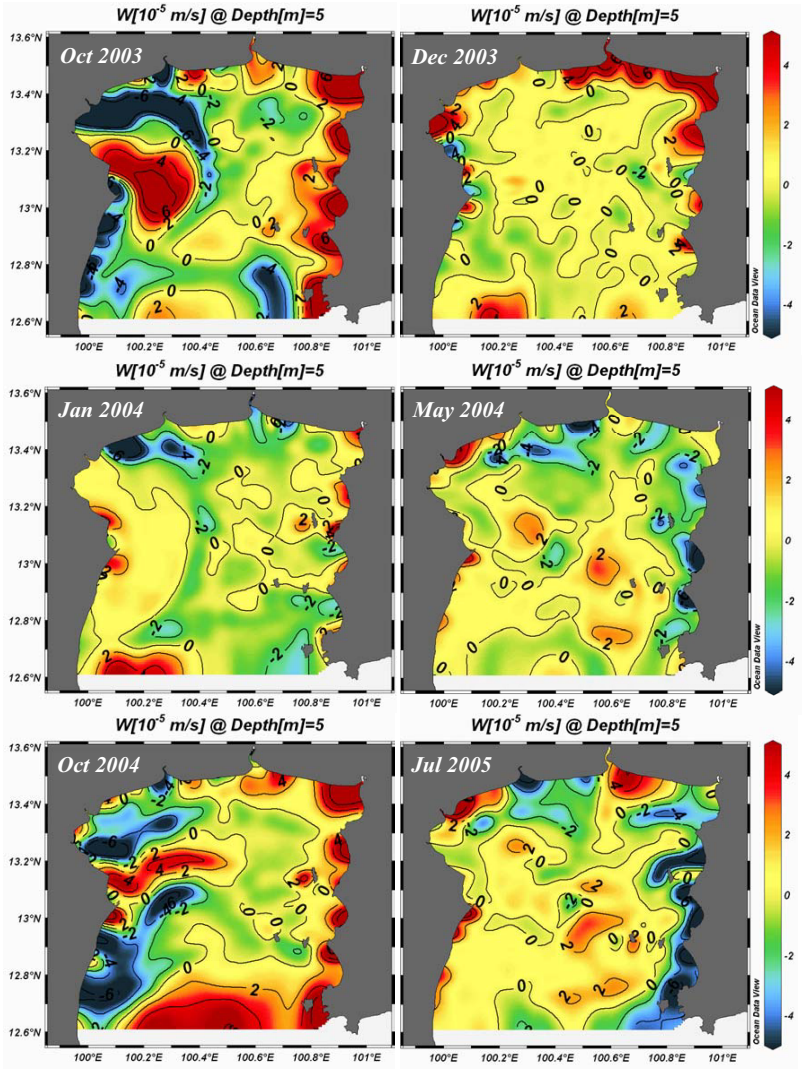

Fig. 5. Simulated vertical velocity in the same months as all cruises.

operation (t = 0). Time steps were 10 s and 300 s for the external and the internal modes, respectively. The model was driven by all driving forces from the start until a quasi-steady state was reached at day 10, which is determined by checking the series of averaged kinetic energy. Since monthly averaged wind and discharge data were used, computed circulations for 30 days after day 20 were averaged to present as residual circulations to compromise such input data. The model was individually operated for the same months of each cruise (Table 1): October 2003, December 2003, January 2004, May 2004, October 2004 and July 2005.

Surface currents follow prevailing winds (Fig. 3) in three major directions; northeast, southwest, and southeast. The northeast winds (October 2003 and 2004, and December 2003) induce strong westward and southward currents along the northern and the western coasts, respectively (Fig. 4). Reverse flows to these patterns result when southwest winds prevail in May 2004 and July 2005. Weak southeast winds in January 2004 generated weak northward and westward flows along the eastern and the northern coasts, respectively. The simulated circulation patterns agree well with those of in situ measurements illustrated in Booncherm (1999). Divergence of surface currents is clearly seen near the west coast in October 2003, corresponding to strong upwelling in the same area (Fig. 5). Upwelling in this area during this season is supposed to be induced by surface current divergence, triggered by the shape of the shoreline and wind direction. Similar patterns are also evident in October 2004, but with a smaller magnitude. Upwelling and downwelling are generated along the eastern and the western coasts, re-

Table 3. Parameters used in the ecosystem model and their references.

Definitions	Symbols	Values	Units	Reported values	References
Maximum photosynthetic rate at 0°C	V_m	1.5	day^{-1}	0.05–8.10	Parsons *et al*. (1984)
Half saturation constant for DIN	K_{SN}	1.0	μmol-N l^{-1}	0.04–4.21	Parsons *et al*. (1984)
Half saturation constant for DIP	K_{SP}	0.05	μmol-P l^{-1}	0.008–0.530	O'Connor *et al*. (1975)
Optimum light intensity for phytoplankton	I_{opt}	16.0	$MJ/m^2/day$	1.8–12.0	Parsons *et al*. (1984)
Coefficient	k_T	7.9964			
Respiration rate of phytoplankton at 0°C	R_0	0.02	day^{-1}	0.030–0.051	Di Toro *et al*. (1971)
Natural mortality rate of phytoplankton at 0°C	M_p	0.03	(μmol-N l^{-1} $day)^{-1}$	0.04	Onitsuka and Yanagi (2005)
Maximum grazing rate of zooplankton at 0°C	R_{max}	0.3	day^{-1}	0.3	Kawamiya *et al*. (1995)
Ivlev constant	λ	0.47	$(mgChl\text{-}a/m^3)^{-1}$	0.47	Smayda (1973)
Threshold of phytoplankton in grazing	P^*	0.05	$mgChl\text{-}a/m^3$	0.08–0.09	Kawamiya *et al*. (1995)
Natural mortality rate of zooplankton at 0°C	M_z	0.06	(μmol-N l^{-1}day)$^{-1}$	0.06	Kawamiya *et al*. (1995)
Assimilation efficiency of zooplankton	α_z	0.7		0.7	Onitsuka and Yanagi (2005)
Growth efficiency of zooplankton	β_z	0.3		0.3	Onitsuka and Yanagi (2005)
Bacterial decomposition rate of detritus at 0°C	V_{PN}	0.05	day^{-1}	0.05	Fasham *et al*. (1990)
Sinking velocity of phytoplankton	S_p	10	cm day^{-1}	33	Smayda (1970)
Sinking velocity of detritus	S_d	100	cm day^{-1}	100	Yanagi *et al*. (1993)

spectively, during the times of the northeast or the southeast winds (October 2003 and 2004, December 2003 and January 2004). Conversely, downwelling occurs along the eastern coast during the southwest monsoon (May 2004 and July 2005). Upwelling along the western coast during this time, however, is ambiguous due to the presence of a sea boundary in the southern part of UGoT. Instead of inducing only surface currents to flow seaward resulting in upwelling of deeper water, the winds partly induce water intrusion though the west area of the sea boundary.

4. Ecosystem Model

NPZD (Nutrient-Phytoplankton-Zooplankton-Detritus), a pelagic ecosystem model (Yanagi *et al*., 2001), was selected for this study due to its simplicity. The model has five compartments, rather than the four implied by its NPZD name, because nutrients are separated into dissolved inorganic nitrogen (DIN) (ammonia + nitrate + nitrite) and dissolved inorganic phosphorous (DIP) (phosphate). Silicate, another important nutrient for some plankton species such as diatom, is not considered in the model system because the study focuses on chl-a distributions, which are independent of plankton species. Diatom, however, is also found to bloom, but only to a minor extent as compared to the dinoflagellates. Mathematical descriptions of the ecosystem model are detailed in Appendix.

Because relevant parameters, especially the physiological properties of plankton in the study area, have rarely been reported, it was necessary to use data measured in other regions, or as applied to other ecosystem model experiments. Table 3 summarizes all parameters used in the ecosystem model, with their previously reported values and references. Most are in ranges of the reported values but some are not, due to the need to keep the results of the chl-a concentration within observed ranges.

Chl-a, DIN and DIP at all major river mouths were required, but no such data were collected during the times of field observations. Therefore, data from the closest stations to each river mouth were applied for this purpose instead. Nutrient concentrations might be inappropriate to represent levels found at the river mouths because of the distances between the reference and the measured points. Accordingly, sensitivity analysis to nutrient variation at the river mouths (Section 6) was conducted to investigate the response of the system to this potential effect.

For the sea boundary, chl-a, DIN and DIP at all cross-sectional grids were derived from extrapolation and interpolation of data of the stations close to the boundary line. The function for two-dimensional approximations (Eqs. (2) and (3)) was applied for this process. The model also needed phytoplankton and detritus data at the open boundary, but neither data were available. Based on energy transfer in the trophic level system (Nybakken and Bertness, 2004), which is also applied to the biomass, zooplankton was assumed to be 10% of phytoplankton biomass while organic detritus was assumed to be equal to phytoplankton biomass. These assumptions were also applied at the river boundaries and initial conditions of model simulation.

Due to data unavailability, averaged solar radiation measured at the Bangkok meteorological station in years 1993 to 2000 (Fig. 6) was used as the radiation over UGoT to calculate underwater light intensity (Eq. (A.12)). High

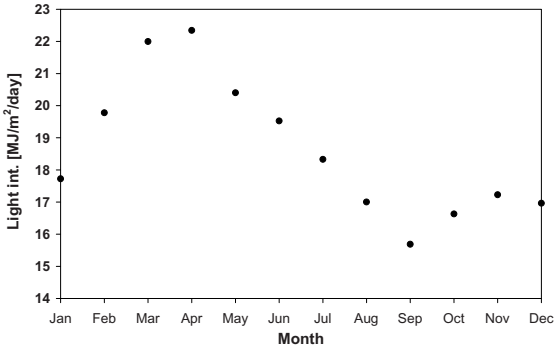

Fig. 6. Averaged monthly light intensities of the data from 1993 to 2000 measured at the Bangkok meteorological station.

and low radiation periods occur from March to June and October to December, respectively, with the annual average as high as 18.64 MJ $m^{-2}d^{-1}$.

The computational domain, grid spacing and time steps were the same as those of POM. Lateral sea boundary conditions of ecosystem parameters P, Z, N_N, N_P and D were the same as those of temperature and salinity with fixed values at all grid locations along the boundary plane throughout model operation. Exchange fluxes of those parameters at the sea surface and bottom boundaries were not permitted because they were unknown, but were assumed to be small compared to the river loads. However, they were set to be recycled in the system until transported out through the sea boundary. The loads of major rivers were taken into consideration, while non-point source nutrients along coastlines were ignored due to a lack of reliable data. Here DIN and DIP loads presented in Fig. 7 were calculated by the multiplication of monthly averaged discharges and their concentrations at the river boundaries.

Initial values of ecosystem parameters, derived from the overall average of measured data, were set to be identical in all experiments –1.65 mg m^{-3}, 10.70 μM-N l^{-1} and 0.33 μM-P l^{-1} for chl-a, DIN and DIP, respectively. Zooplankton and detritus were assigned as 10% of chl-a and equal to chl-a concentrations, respectively, similar to the lateral boundary setting.

When using this computational technique, the units of all parameters have to agree, so μM-N l^{-1} was selected as the standard unit for this experiment. The Redfield mole ratio of C:N:P (=106:16:1) (Redfield *et al*., 1963) and the C:chl-a mass ratio (=50) (Parsons *et al*., 1984) are major converters to modify parameter units. Values of the ratios differ on an area-by-area basis due to dominant plankton species and their physiological properties. However, it was appropriate to apply the standard values in order to compare the seasonal variations of chl-a distributions when local environmental factors have changed.

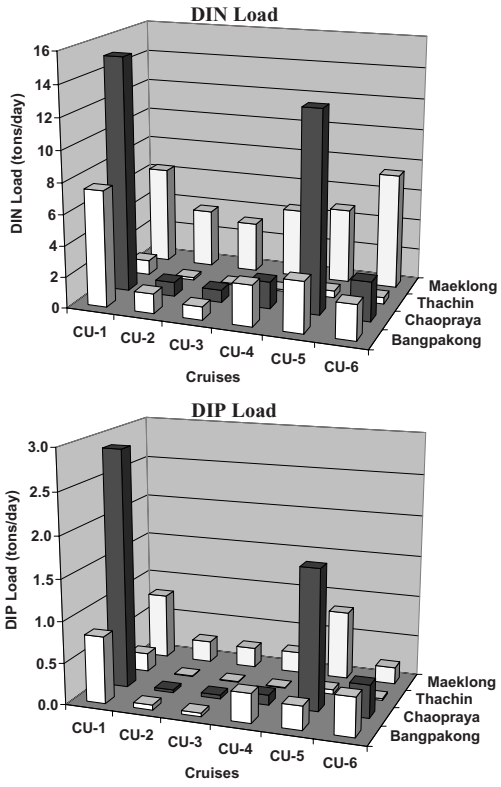

Fig. 7. Monthly averaged DIN and DIP loads of major rivers.

The model operation was tested and a steady state of all simulated parameters was attained after days 10 of computation. Calculated results were collected and averaged from days 20 to 50 in the same way as those of circulation model. Simulated chl-a distributions in the same months of observational cruises are presented and discussed.

5. Simulated Surface Chl-a Distributions

High chl-a water always appears downwind, or in the same direction as the surface current (Fig. 8). Currents along the northern coastline moving to the west induce high chl-a concentrations along the west coast in October 2003 and 2004, December 2003 and January 2004. On the other hand, when currents change by moving to the east in May 2004 and July 2005, dense plankton areas result. These phenomena are explained by the movement of nutrient sources from the rivers after discharge into water at the head of UGoT. Currents along the northern coast play an important role in moving those nutrients eastward and westward in relation to seasons (Figs. 9 and 10). Phytoplankton in this part of UGoT grows vigorously in areas following these trends. It was observed that the centers of high chl-a concentration are not strictly correlated with the river mouths where the

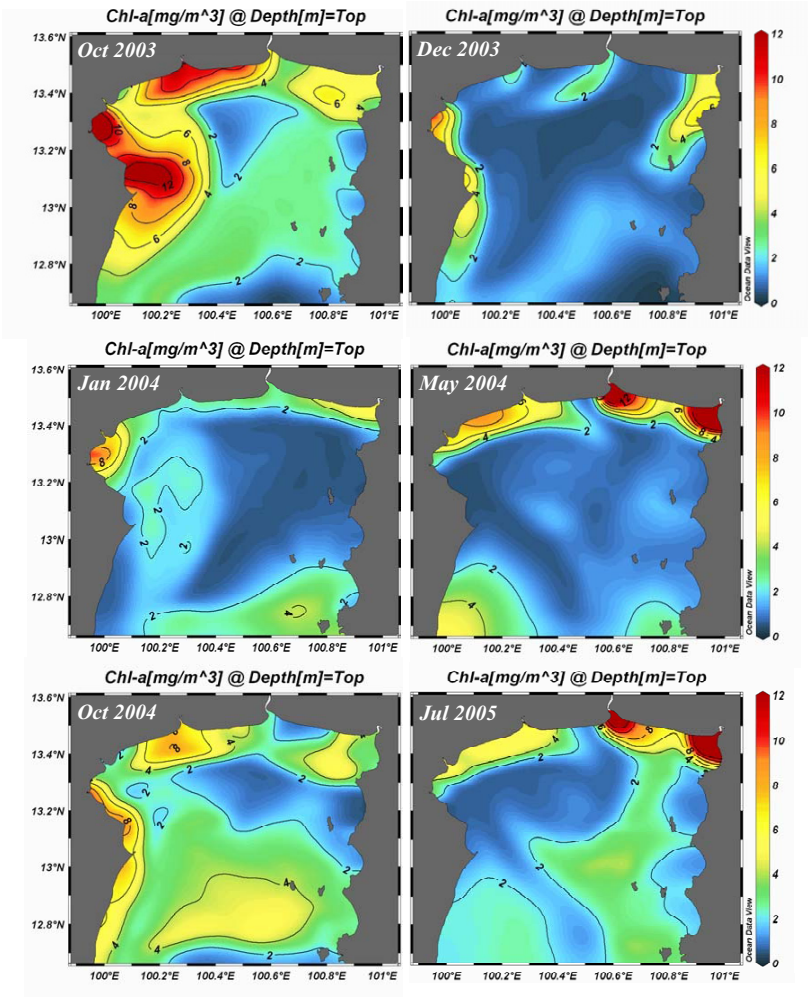

Fig. 8. Simulated chl-a distributions at the sea surface from the reference cases.

nutrients are originally loaded. Because phytoplankton needs a period of time for growth, they are conveyed farther away the river mouths following ambient currents before they reach their peak concentrations. Computed nutrients in those areas are obviously low (Figs. 9 and 10) owing to photosynthetic activity.

Seasonal movement of high chl-a patchiness to the west and the east of UGoT following the northeast and the southwest monsoons, respectively, strongly confirm the importance of river discharges as the most important source of nutrients for phytoplankton photosynthesis in UGoT. If nutrients were supplied from other sources, such as the open boundary in the south, the resulting bloom areas would be completely changed.

Comparisons of simulated chl-a distributions (Fig. 8) with those of field observations (Fig. 11) show consistency in the spatial variation of plankton blooming in October 2003. High simulated chl-a in the middle of the west coast corresponds to strong upwelling (Fig. 5) and low vertical diffusivity (Fig. 12) around that region in October 2003. Both factors play an important role in helping to stabilize plankton cells near the sea surface, thereby increasing photosynthetic rates. The water brought to the surface through upwelling does not contribute nutrients since bottom fluxes are not permitted in the model. In addition, nutrient concentrations are uniform throughout the water column due to shallowness and good vertical mixing. The explanation of weak blooming incidents in October 2004, compared to October 2003, is related to weak upwelling and strong vertical diffusivity at that time. Nutrients in the water column may not be a limiting factor for phytoplankton bloom in UGoT because, based on Eqs. (A.9) and (A.10), the half saturation constants (K_{SN} = 1 μM-N l^{-1} and K_{SP} = 0.05 μM-P l^{-1}) are very low compared to nutrient concentrations (Figs. 9 and 10). Nutrients are therefore considered to be sufficient to sup-

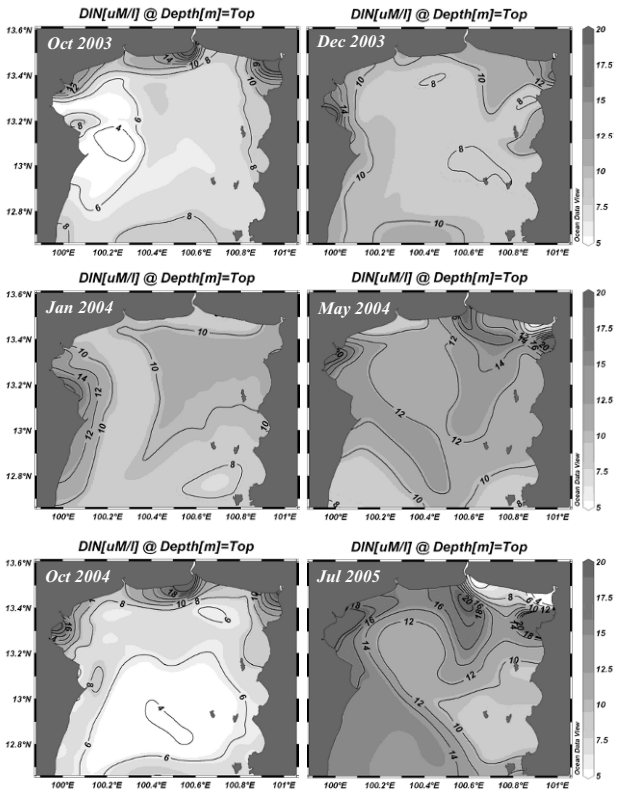

Fig. 9. Simulated DIN distributions at the sea surface from the reference case.

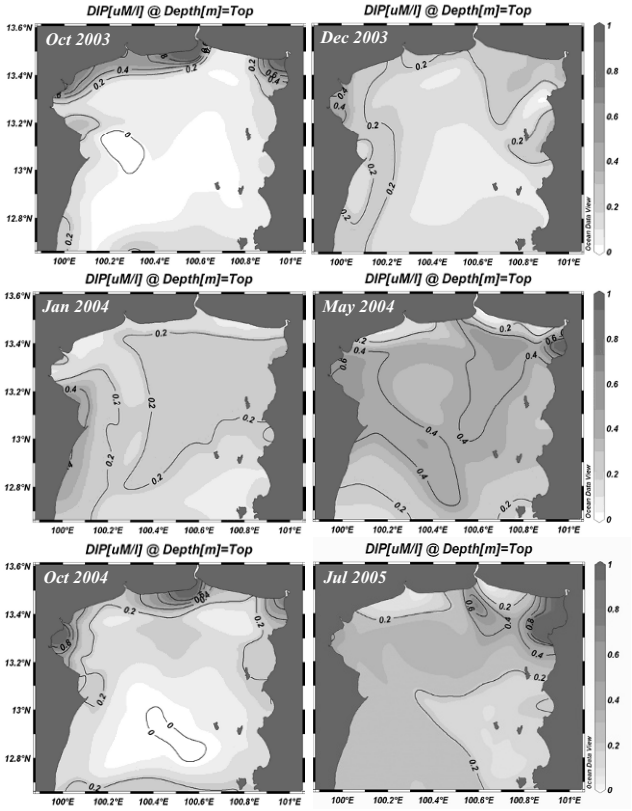

Fig. 10. Simulated DIP distributions at the sea surface from the reference cases.

port plankton blooms in the whole area all year round.

Seasonal variations in vertical diffusivity are still unclear as to what major factors control this phenomenon. A rough explanation can be that tidal propagation in UGoT is counterclockwise (Anongponyoskun, 2006). Wind-driven current, if it follows this movement trend, will be associated with small turbulence. If not, strong turbulence will be generated due to oppositely directed current propagation. Therefore, low turbulence usually occurs during the northeast wind, while high turbulence is generated during the southwest wind. The variations are so complicated because this phenomenon is sensitive to wind direction, wind magnitude, water conditions (e.g., stratification), heat flux and river discharges, to give some examples. We intend to focus on the issue of seasonal variations in diffusivity and turbulence in UGoT in our next study, using both field observation and a numerical model.

Chl-a distribution models for May 2004 and July 2005 (Fig. 8) are both discussed because these periods of time are influenced by the southwest wind. They all illustrate the same trend of movement of high chl-a to the east coast following the southwest wind and east current along the northern shoreline. High concentration seems to remain very close to the shoreline, especially in the northeast area. The limit of high chl-a concentration is likely to be controlled by the vertical diffusivities (Fig. 12) described above. The measured chl-a plots during Cruise CU-4 (12–15 May 2004) agree with this chl-a movement, while those during Cruise CU-6 (26–28 July 2005) do not. This may be explained for two reasons. First, scattered measurement points may not cover a high chl-a area located close to the northern coastline. Second, temporal changes in wind speed might be the cause of strong turbulence and thus low chl-a at that time. The mean wind magnitude during Cruise CU-6 was 8.1 m s^{-1} (Matsumura *et al*., 2006), while the monthly mean wind magnitude in the same month from QuickScat, forced in the model, was just 6.3 m s^{-1}. The difference in wind strength between both situations may play a key role in explaining such chl-a variations.

Disagreement with the observed results was also seen in December 2003, when the ecosystem model cannot reproduce blooming near the northwest coast as observed with the field data. No massive growth of phytoplankton is given by the model simulation due to high vertical diffusivity induced by wind (Fig. 12). High chl-a during Cruise CU-2 (4–6 December 2004) might be triggered by

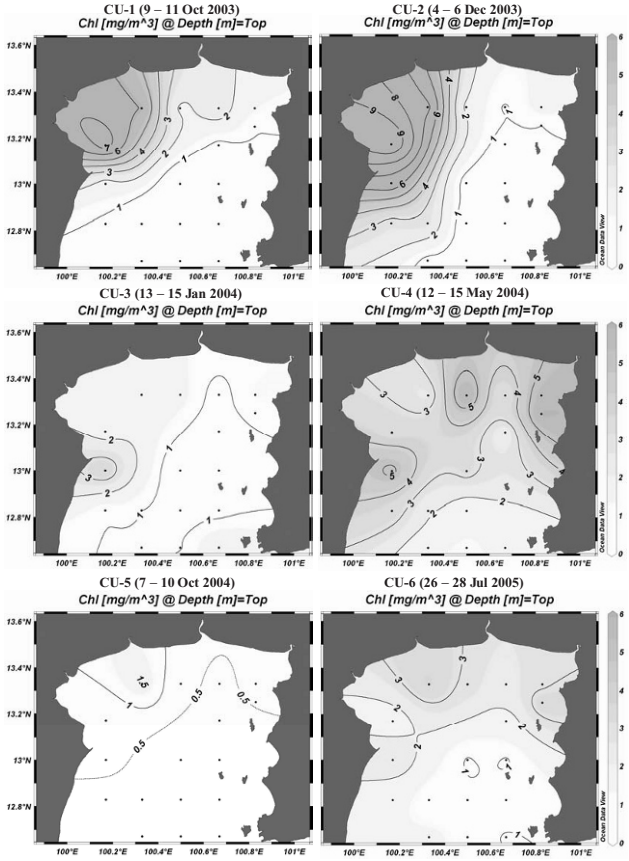

Fig. 11. Horizontal distributions of chl-a at the sea surface of the data from field observations. Dots represent observation stations.

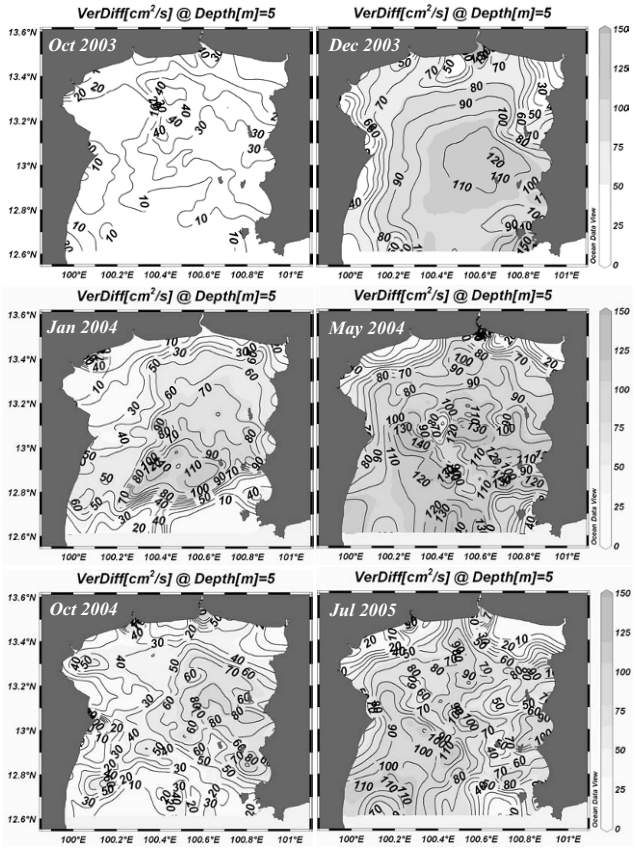

Fig. 12. Simulated vertical diffusivities at 5 m depth from the reference cases.

a weak wind of 3.9 m s^{-1} measured during the cruise period (Matsumura *et al*., 2006). Simulated chl-a was not high because the monthly mean wind forced in the model (7.0 m s^{-1}) was almost twice as large as the actual measurement during the cruise period. The relationship between wind magnitude and chl-a concentration is examined in Section 6.

Understanding the relationship between water turbulence and plankton growth from the numerical experiment is used to explain why simulated chl-a was usually higher than the measured value. The model takes just wind, tide, and river discharge as significant forces driving water circulation. The model does not include waves because their influence on water circulation in the study area is minor. Wave action, however, plays a significant role in increasing turbulence or mixing, especially at the sea surface. Turbulence in real situation is presumably larger than that generated in the model simulation. Since calm water favors phytoplankton growth, simulated chl-a is then higher than the observed value. Further investigations are urgently required to validate this hypothesis.

6. Sensitivity Analyses

The sensitivities of simulated chl-a to varying nutrient loads and wind magnitudes are investigated and discussed here. Since nutrient loads can be modified by changing either nutrient concentration or discharge data, these two approaches are both tested separately. The sensitivity to wind magnitude is included because of its influence on vertical current and diffusivity, and previous results indicate that high concentrations of chl-a are spatially restricted to areas of upwelling or low vertical diffusivity. Based on this, the patterns of chl-a distribution should change if wind magnitudes are varied.

The tested factors were set to be 50% larger and smaller than those in the reference cases, while model setting and operation were the same as in the reference simulations. Differences in simulated values of surface chl-a, after nutrients at the river boundaries, discharges, and wind velocities were increased/decreased, are plotted to investigate the level of influence of these factors on chl-a variations (Figs. 13(a) and (b)). All values are positive because they were derived from the absolute sub-

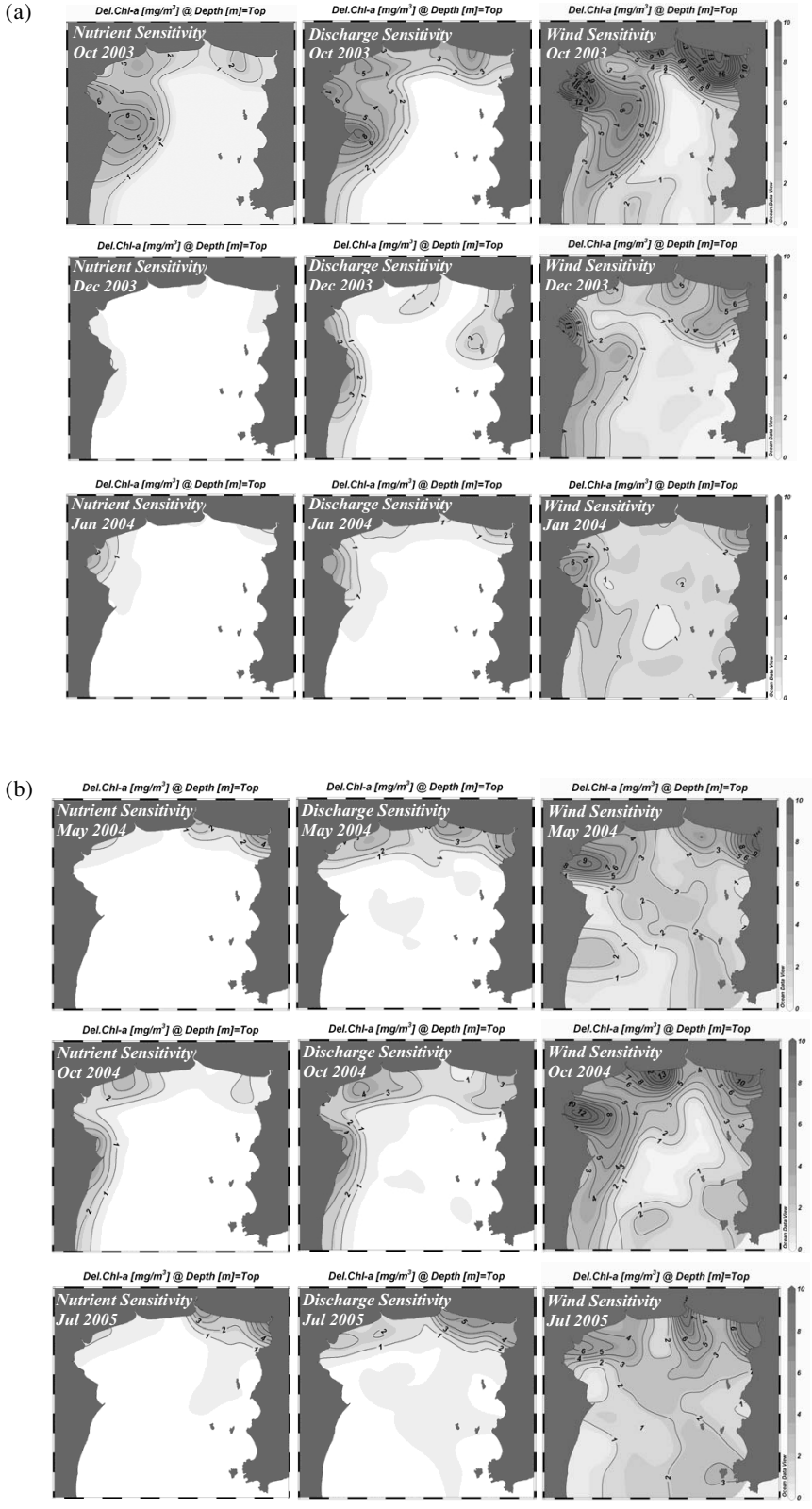

Fig. 13. (a) Differences of simulated surface chl-a after nutrients at the river mouths, river discharges, and wind velocities were increased and decreased by 50% in October 2003, December 2003 and January 2004. (b) As (a) but in May 2004, October 2004 and July 2005.

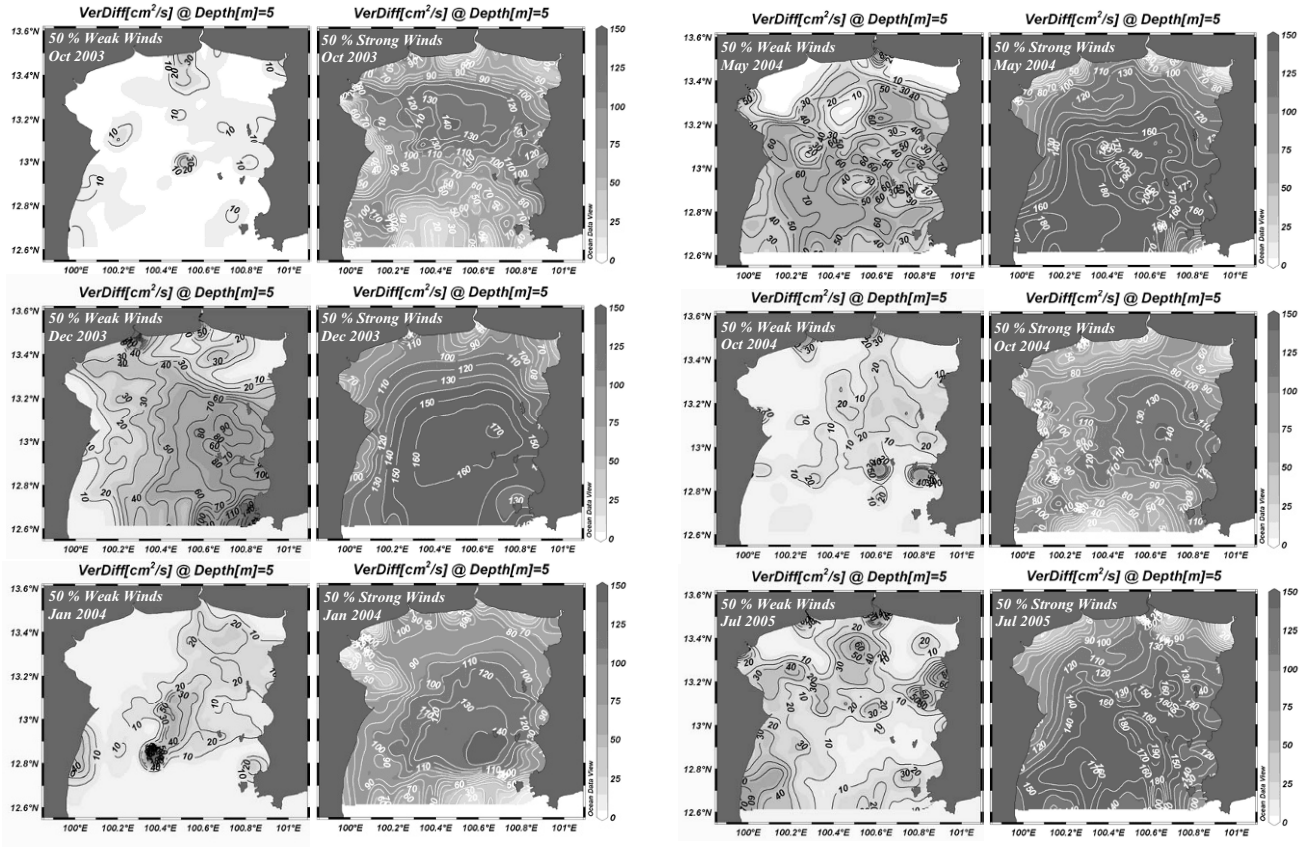

Fig. 14. (a) Vertical diffusivities at 5 m depth under simulated weak and strong winds in October 2003, December 2003 and January 2004. (b) As (a) but in May 2004, October 2004 and July 2005.

traction between two scenarios of high and low chl-a cases. Chl-a distributions in all seasons are most sensitive to wind variations. Changes in wind magnitude strongly change both the intensity and distributions of blooms. Sensitivity to changes in nutrient loads through concentration and discharge only increase chl-a intensity, not blooming areas. Sensitivity analysis also supports the importance of nutrients in primary production. Although the blooming area is not expanded, as in the case of wind sensitivity, chl-a concentration over the same blooming area is intense when the nutrient river loads increase (e.g., Fig. 15).

The analysis reveals the relationship between wind magnitude, related to vertical diffusivity or stability condition, and chl-a distributions in this area. High chl-a water is geographically bounded within the area of low vertical diffusivities (Fig. 12), although high nutrient areas have a greater spatial extent (Figs. 9 and 10). Water stability is also increased by buoyancy fluxes from river water; therefore, plankton blooms are usually found near the river mouths. The influence of river discharge, however, does not result in large chl-a variations because strong vertical mixing due to wind overwhelms their influence. Wind speed plays a crucial role in controlling vertical diffusivities, which is clearly seen in Figs. 14(a) and (b). Decreases in wind velocities, resulting in reduction of vertical diffusivities, increase the chance of plankton photosynthesis and surface chl-a accumulation. Alternatively, when wind speed and vertical mixing are strong, the blooming area is shrunk (e.g., Fig. 15). This explanation and the example also support evidence of blooming and non-blooming due to temporary weak wind and strong wind during Cruises CU-2 and CU-6, respectively, as discussed in Section 5.

The occurrence of year-to-year variations in plankton blooms between October 2003 and October 2004 is uncovered by sensitivity experiments on wind variability. Nutrient loads are high at time of the year (Fig. 7), but intense plankton blooming occurs in October 2003 but not in October 2004 (Fig. 8). It is possible that a strong bloom in October 2003 is the result of smaller vertical diffusivity and stronger upwelling along the western coast,

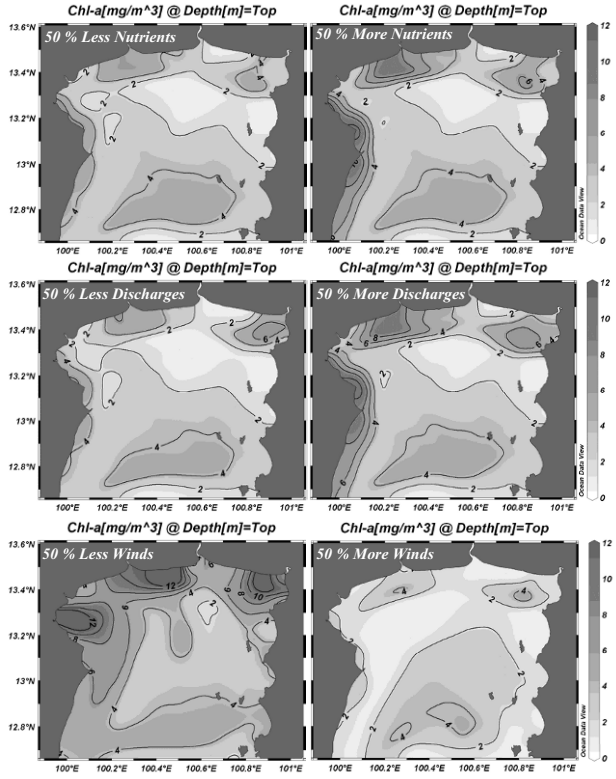

Fig. 15. Responses of simulated surface chl-a distributions to variations of river nutrients, discharges and wind magnitudes in October 2004.

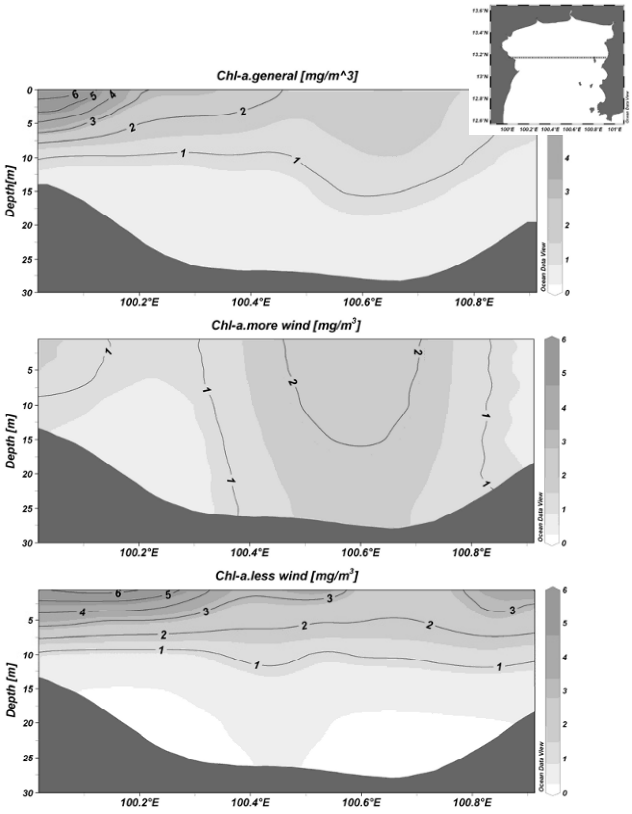

Fig. 16. Vertical chl-a distributions of reference condition and simulated results when wind speeds were increased and decreased by 50% in October 2004.

corresponding to larger river discharges and characteristic of wind fields, respectively. River discharge has a potential to reduce vertical diffusivity by increasing water stability through buoyancy flux. With regard to upwelling, winds in October 2003 approached a more easterly direction than those in October 2004, while their magnitudes were almost the same. Such wind directions in the former year, characteristic of the western coastline, may trigger strong surface divergence (Fig. 4), resulting in strong upwelling (Fig. 5) around that area in October 2003. This phenomenon was not prominent in October 2004, when the winds mostly generated southward flow and weak divergence. Interestingly, after the wind magnitude has decreased, blooming regions occur almost the same as those in October 2003 (Fig. 15). Nutrient load increases, however, can just increase chl-a intensity over the same extent. Vertical chl-a distributions along an east-west transverse line in October 2004 (Fig. 16) strongly support this by illustrating a great accumulation of chl-a near the sea surface when wind speed decreases. The results verify the critical role of the stability condition (low vertical diffusion or mixing) on the water column in plankton growth, which can be used to explain this annual variation successfully.

Monthly averaged wind, applied as a major forcing in the ecosystem model, might not represent the actual conditions of short-term wind variations. Actual wind speeds in nature are not always stable, and do not fix in the same direction all the time. They are variable in intensity and direction due to local influences of sea breeze or land breeze, depending on time of day and season. Alternating strong and slack wind-induced turbulence in the water column might alternate phytoplankton growth. Strong mixing reduces, while calm periods increase phytoplankton abundance. The balancing of lengths of time when these conditions persist might play a key role in determining plankton dynamics. We shall conduct separate research regarding wind issues on chl-a and primary productivity in this area in the near future.

A survey of the UGoT area indicates that red tides usually occur after rainfall coupled with strong sunshine (Lirdwitayaprasit *et al*., 2006). Sensitivity analysis clarifies the mechanism of phytoplankton bloom in such conditions. Nutrients in the system might be increased by larger river discharges due to precipitation, contributing to increased fertility of the water column. However, in-

creases of nutrient load only are not enough to increase chl-a. Water stability and sunlight are still required to initiate plankton blooming. Coincidently, slack wind and calm water, lasting about 2–3 days, usually come after the rain. Moreover, falling rain might help to increase water stability by adding buoyancy flux at the sea surface. If there is enough sunlight during such calm conditions, the opportunity to bloom will increase, especially in the vicinity of the river mouths and where the nutrient loads are transported. This mechanism is very interesting and warrants further attention.

7. Conclusion

The NPZD ecosystem model coupled with POM has been used to investigate surface chl-a distributions in the UGoT. The results clearly indicate that seasonal variations in chl-a distributions are related to winds, currents and nutrient loads from the rivers. High chl-a patchiness is located near the western coast following the direction of westward circulation developed during the northeast monsoon while the accumulation of high concentration could be observed around the northeastern coast due to eastward flow during the southwest monsoon. The intensity of plankton blooming near the coasts and the river mouths is proportional to nutrient loads, while in offshore areas, vertical movement and stability of the water column are crucial in addition to nutrients. Chl-a will be high wherever vertical diffusivity is low, or upwelling occurs. The experiments also reveal that strong vertical mixing prevents surface phytoplankton accumulation, even in fertile water.

Sensitivity analysis has demonstrated that factors with the greatest influence on chl-a distribution in the study area are variations in wind speeds. Nutrient loads through river discharge modification contribute primarily to the intensity of plankton blooms, but not significantly to their spread. Sensitivity experiments in the case of wind variability have demonstrated the occurrence of year-to-year variation in plankton blooms between October 2003 and October 2004. Nutrient loads in both periods were similarly high, but blooming occurred in the former case only due to strong upwelling and low diffusivity induced by winds. Massive plankton growth, such as that in October 2003, could be reproduced by decreasing wind magnitudes in October 2004.

Acknowledgements

The authors would like to thank Dr. Mark Flaherty of the University of Victoria, Dr. Pichan Sawangwong and Dr. Kashane Chalermwat of Burapha University, and Dr. Thithaworn Lirdwittyaprasit of Chulalongkorn University for their support and comments; researchers and students of the Department of Marine Science, Chulalongkorn University for their hard work in the fields for data collection; Royal Irrigation Department, Pollution Control Department and Meteorological Department of Thailand for providing ancillary data used in numerical models. The field campaigns were financially supported by the Japan Society for the Promotion of Science (JSPS), the Japan International Cooperation Agency (JICA) and the National Research Council of Thailand (NRCT). Gratitude is also expressed to two anonymous reviewers and Dr. Joji Ishizaka, Nagasaki University for their fruitful comments and suggestions to shape up this manuscript.

Appendix

The ecosystem model of five compartments, including phytoplankton (P), zooplankton (Z), detritus (D), DIN (N_N) and DIP (N_P), is incorporated into five governing equations (Guo and Yanagi, 1998), expressed in a Cartesian coordinate system, shown as follows:

$$\frac{\partial P}{\partial t} + \vec{V} \cdot \nabla P + S_P \frac{\partial P}{\partial z} = DIF(P) + A_1 P - R_1 P - A_2 P^2 - A_3 Z, \tag{A.1}$$

$$\frac{\partial Z}{\partial t} + \vec{V} \cdot \nabla Z = DIF(Z) + A_3 Z - A_4 Z^2 - A_5 Z - A_6 Z, \tag{A.2}$$

$$\frac{\partial D}{\partial t} + \vec{V} \cdot \nabla D + S_d \frac{\partial D}{\partial z} = DIF(D) + A_2 P^2 + A_4 Z^2 + A_6 Z - A_7 D, \tag{A.3}$$

$$\frac{\partial N_N}{\partial t} + \vec{V} \cdot \nabla N_N = DIF(N_N) - A_1 P + A_6 Z + A_7 D, \tag{A.4}$$

$$\frac{\partial N_P}{\partial t} + \vec{V} \cdot \nabla N_P = DIF(N_P) - A_1 P + A_6 Z + A_7 D, \tag{A.5}$$

where

$$\vec{V} \cdot \nabla(\ ) = u \frac{\partial}{\partial x} + v \frac{\partial}{\partial y} + w \frac{\partial}{\partial z}, \tag{A.6}$$

$$DIF(\ ) = \frac{\partial}{\partial x}\left(K_h \frac{\partial}{\partial x}\right) + \frac{\partial}{\partial y}\left(K_h \frac{\partial}{\partial y}\right) + \frac{\partial}{\partial z}\left(K_v \frac{\partial}{\partial z}\right). \tag{A.7}$$

Here $\vec{V}$ is three-dimensional velocity composed of u, v, and w, which are velocity components in x, y and z directions, respectively; x and y are axes in the horizontal plane, and z is that in the vertical direction; t is time; and K_h and K_v are horizontal and vertical diffusivities, respectively.

Velocity and diffusivity data used in the ecosystem model are the results of POM computed in the same time step. S_p and S_d, sinking speeds of phytoplankton and detritus, respectively, are set as constants. The biochemical terms are described below, and all relevant parameters are summarized in Table 3.

Phytoplankton growth rate A_1 is decided by:

$$A_1 = V_m k_T \min\{V_1(N_N), V_1(N_P)\} \cdot V_2(I), \quad \text{(A.8)}$$

$$V_1(N_N) = \frac{N_N}{K_{SN} + N_N}, \quad \text{(A.9)}$$

$$V_1(N_P) = \frac{N_P}{K_{SP} + N_P}, \quad \text{(A.10)}$$

$$V_2(I) = \frac{I}{I_{opt}} \exp\left(1 - \frac{I}{I_{opt}}\right). \quad \text{(A.11)}$$

Considered in terms of the Redfied ratio, most observed N/P mole ratios of over 16 indicate that DIP might be the limiting nutrient. The model, however, allows both nutrients to control phytoplankton growth, depending on their simulated concentrations in the computational domain. I is the light intensity at a given depth which is expressed as:

$$I(z) = I_s \exp\left[-\int_0^z k(z)\,dz\right], \quad \text{(A.12)}$$

$$k(z) = 0.04 + 0.054C(z)^{2/3} + 0.0088C(z), \quad \text{(A.13)}$$

$$C(z) = P(z) + \delta(Z(z) + D(z)), \quad \text{(A.14)}$$

where I_s denotes the light intensity at the sea surface; k is the extinction coefficient; and C is the concentration of chl-a. Self-shading, a phenomenon contributing to decreased underwater light resulting from suspended plankton cells and other organic particles, is represented by Eq. (A.13) (Riley, 1956). Not only phytoplankton, but also zooplankton and detritus are considered in the self-shading effect (Eq. (A.14)), where δ is a constant representing the contribution of those non-algal particles. It should be added that the water column near the river mouths is quite turbid, with strong seasonal variations following river discharge, monsoonal wind and current. The influence of water turbidity, together with phytoplankton, zooplankton and detritus, on the extinction coefficient, however, has not yet been reported for the UGoT area. Lacking such information, the functions reported in another study, as shown in Eqs. (A.13) and (A.14), were employed in this study.

Temperature and salinity might be included as variables in the growth function A_1 (Eq. (A.8)) if their variations have a strong influence on phytoplankton abundance or distribution. This study considers neither factor because they demonstrate no significant relationship with chl-a.

The coefficient k_T is derived from a function $\exp(k_0 \cdot T)$, where k_0 is a constant 0.0693 (Kawamiya *et al*., 1995) and T is water temperature in °C. Here T was set to 30°C, which is consistent with observed data; therefore, k_T = 7.9964. k_T is based on the rate of change of photosynthesis to temperature (Eppley, 1972). It was also adopted for other physiological processes that depend on temperature, as shown below. This application has successfully been applied in several studies, such as those of Kawamiya *et al*. (1995) and Onitsuka *et al*. (2007).

The respiration rate of phytoplankton R_1:

$$R_1 = k_T R_0. \quad \text{(A.15)}$$

The natural mortality rate of phytoplankton A_2:

$$A_2 = k_T M_p. \quad \text{(A.16)}$$

The grazing rate of zooplankton A_3:

$$A_3 = k_T R_{\max}[1 - \exp \lambda(-P + P^*)]. \quad \text{(A.17)}$$

When phytoplankton concentration (P) is smaller than the threshold of phytoplankton in grazing (P^*), A_3 is set to zero, which means phytoplankton will not be eaten if its concentration is below the grazing threshold.

The natural mortality rate of zooplankton A_4:

$$A_4 = k_T M_z. \quad \text{(A.18)}$$

The production rate of fecal pellets of zooplankton A_5:

$$A_5 = (1 - \alpha_z) \cdot A_3. \quad \text{(A.19)}$$

The generation rate of urine of zooplankton A_6:

$$A_6 = (\alpha_z - \beta_z) \cdot A_3. \quad \text{(A.20)}$$

The decomposition rate of detritus A_7:

$$A_7 = k_T V_{PN}. \quad \text{(A.21)}$$

References

Anongponyoskun, M. (2006): Tide around Loi Island, Sriracha, Chonburi Province. *Burapha Science Journal*, **11**(1), 40–46 (in Thai with English abstract).

Blumberg, A. F. and G. L. Mellor (1987): A description of a three-dimensional coastal ocean circulation model. p. 1–16. In *Three-Dimensional Coastal Ocean Models, Coastal and Estuarine Sciences*, 4, ed. by N. S. Heaps, AGU, Washington, D.C.

Booncherm, C. (1999): The seasonal cycle of residual flows and the tidal currents in the Gulf of Thailand by using the long-term observed data from the SEAWATCH Thailand Program. M.Sc. Thesis, Department of Ocean Science, University of Wales, Bangor.

Bunpapong, M. and T. Piyakarnchana (1987): Some trend in the upper Gulf water quality. *Proceedings of the 4th Seminar on Water Quality and Living Resources in Thai Water*, 270–283.

Buranapratheprat, A., T. Yanagi and P. Sawangwong (2002): Seasonal variations in circulation and salinity distributions in the upper Gulf of Thailand: modeling approach. *La mer*, **40**, 147–155.

Chalermwat, K. and R. A. Lutz (1989): Farming the Green Mussel in Thailand. *World Aquaculture*, **20**, 41–46.

Chongprasith, P. and V. Srineth (1998): Marine water quality and pollution of the Gulf of Thailand. p. 137–204. In *SEAPOL Integrated Studies of the Gulf of Thailand*, Vol. 1, ed. by D. M. Johnston, Southeast Asian Programe in Ocean Law, Policy and Management.

Di Toro, D. M., D. J. O'Connor and R. V. Thomann (1971): A dynamic model of the phytoplankton population in the Sacramento-San Joaquin Delta, Nonequilibrium systems in natural water chemistry. *Adv. Chem. Ser.*, **106**, 131–180.

Eppley, R. W. (1972): Temperature and phytoplankton growth in the sea. *Fishery Bullatin*, **70**, 1063–1085.

Fasham, M. J. R., H. W. Ducklow and S. M. McKelvie (1990): A nitrogen-based model of plankton dynamics in the ocean mixed layer. *J. Mar. Res.*, **48**, 591–639.

Guo, X. and T. Yanagi (1998): The role of Taiwan Strait in an ecological model in the East China Sea. *Acta Oceanographica Taiwanica*, **37**(2), 139–164.

Kawamiya, M., M. J. Kishi, Y. Yamanaka and N. Suginohara (1995): An ecological-physical coupled model applied to Station Papa. *J. Oceanogr.*, **51**, 635–664.

Kourafalou, V. H., L. Y. Oey, J. D. Wang and T. N. Lee (1996): The fate of river discharge on the continental shelf 1. Modeling the rive plume and the inner shelf coastal current. *J. Geophys. Res.*, **101**, 3415–3434.

Lirdwitayaprasit, T., T. Vicharangsan and N. Sawetwong (1994): Occurrences of red tide phenomena in the inner Gulf of Thailand during 1991–1994. *Proceedings of the First NRCT-JSPS Joint Seminar on Marine Science*, 106–110, Chulalongkorn University Printing House, Bangkok.

Lirdwitayaprasit, T., S. Meksumpun, S. Rungsupa and K. Furuya (2006): Seasonal variations in cell abundance of *Noctiluca scintillans* in the coastal waters off Chonburi Province, the upper Gulf of Thailand. *Coast. Mar. Sci.*, **30**(1), 80–84.

Matsumura, S., A. Siripong and T. Lirdwitayaprasit (2006): Underwater optical environment in the upper Gulf of Thailand. *Coast. Mar. Sci.*, **30**(1), 36–43.

Mellor, G. L. (1998): User's Guide for a Three-Dimensional, Primitive Equation, Numerical Ocean Model. Program in Atmospheric and Oceanographic Sciences Report, Princeton University, Princeton, N.J., 41 pp.

Nybakken, J. W. and M. D. Bertness (2004): *Marine Biology: An Ecological Approach*. 6th ed., Benjamin Cummings, CA, 592 pp.

O'Connor, D. J., D. M. Di Toto and R. V. Thomann (1975): Phytoplankton models and eutrophication problems. In *Ecological Modeling in a Resource Management Framework*, ed. by C. S. Russell, Resources for the Future, Washington, D.C.

Onitsuka, G. and T. Yanagi (2005): Differences in ecosystem dynamics between the northern and southern parts of the Japan Sea: Analyses with two ecosystem models. *J. Oceanogr.*, **61**, 415–433.

Onitsuka, G., T. Yanagi and J.-H. Yoon (2007): A numerical study on nutrient sources in the surface layer of the Japan Sea using a coupled physical-ecosystem model. *J. Geophys. Res.*, **112**, C05042, doi:10.1029/2006JC003981.

Parsons, T. R., M. Takahashi and B. Hargrave (1984): *Biological Oceanographic Processes*. 3rd ed., Pergamon, 330 pp.

Piemsomboon, A. (2003): Influential factors on phytoplankton abundance and toxicity. p. 43–54. In *Red Tide Monitoring in the Gulf of Thailand*, ed. by ARRI, Aquatic Resources Research Institute, Chulalongkorn University and Water Quality Management Section, Pollution Control Department, Bangkok (in Thai).

Piyakarnchana, T., N. Paphavasit, G. Wattayakorn and M. Bunpapong (1990): Marine pollution in the Gulf of Thailand. p. 44–75. In *Land-Based Marine Pollution Problems in the Asia-Pacific Region: Status and Legal Development*, ed. by T. Piyakarnchana, V. Muntabhorn and D. M. Johnson, Institute of Asia Studies, Chulalongkorn University, Bangkok.

Redfield, A. C., B. H. Ketchum and F. A. Richards (1963): The influence of organisms on the composition of seawater. p. 26–77. In *The Sea, Ideas and Observations on Progress in the Study of the Seas*, Vol. 2, ed. by M. N. Hill, Interscience.

Riley, G. A. (1956): Oceanography of Long Island Sound, 1952–1954, II. *Phys. Oceanogr. Bull. Bing. Ocean. Coll.*, **15**, 15–46.

Rungsupa, S., C. Throngroop, A. Piemsomboon, N. Paphawasit, A. Panichphon and A. Sophol (2003): Red tide incidences in the Gulf of Thailand. p. 75–106. In *Red Tide Monitoring in the Gulf of Thailand*, ed. by ARRI, Aquatic Resources Research Institute, Chulalongkorn University and Water Quality Management Section, Pollution Control Department, Bangkok (in Thai).

Smayda, T. J. (1970): The suspension and sinking of phytoplankton in the sea. *Mar. Biol. Annu. Rev.*, **8**, 353–414.

Smayda, T. J. (1973): The growth of *Sceletonema costatum* during a winter–spring bloom in Narragansett Bay. *R.I. Norw. J. Bot.*, **20**, 219–247.

Sojisuporn, P. and P. Putikiatikajorn (1998): Eddy circulation in the upper Gulf of Thailand from 2-D tidal model. *Pro-*

ceedings of the IOC/WESTPAC Fourth International Scientific Symposium, 515–522.

Strickland, J. D. H. and T. R. Parsons (1972): *A Practical Handbook of Seawater Analysis*. Fishery Research Board of Canada, Ottawa, 310 pp.

Tamiyavanich, S. (1984): The causes and impacts of the red tide phenomena occurring in the upper Gulf of Thailand. *Proceedings of the Third Seminar on the Water Quality and the Quality of Living Resources in Thai Waters: 26–28 March 1984*, 481–489, National Research Council of Thailand (in Thai with English abstract).

Wattayakorn, G. (2006): Environmental issues in the Gulf of Thailand. p. 249–259. In *The Environment in Asia Pacific Harbours*, ed. by E. Wolanski, Springer, The Netherlands.

Wiriwutikorn, T. (1996): Long-term variations of nutrients in the upper Gulf of Thailand. M.Sc. Thesis, Inter-Department of Environmental Science, Chulalongkorn University, Bangkok.

Yanagi, T. (1999): *Coastal Oceanography*. TERRAPUB, Tokyo, 162 pp.

Yanagi, T., Y. Mizuno, A. Hoshika and T. Tanimoto (1993): Vertical flow and sinking velocities of particles estimated by a box model in Osaka Bay. *Bull. Coast. Oceanogr.*, **31**, 121–128 (in Japanese with English abstract).

Yanagi, T., G. Onisuka, N. Hirose and J. H. Yoon (2001): A numerical simulation on the mesoscale dynamics of the spring bloom in the Sea of Japan. *J. Oceanogr.*, **57**, 617–630.